Sliding friction: the contribution from defects

1997 J. Phys.: Condens. Matter 9 2869

(http://iopscience.iop.org/0953-8984/9/14/004)

J. Phys.: Condens. Matter **9** (1997) 2869–2889. Printed in the UK PII: S0953-8984(97)77405-8

Sliding friction: the contribution from defects

B N J Persson and A I Volokitin†

Institut für Festkörperforschung, Forschungszentrum Jülich, D-52425 Jülich, Germany

Received 27 August 1996, in final form 8 January 1997

Abstract. We study the influence of defects on the sliding friction for one-, two-, and three-dimensional elastic solids. We show that for 1D and 2D solids, perturbation theory breaks down at low sliding velocity. For a 1D solid with a low concentration of point defects we present an exact solution for the sliding friction, valid for arbitrary temperature and strength of the defect potential. We discuss the role of point defects in the linear (in the external driving force) sliding friction for Xe monolayers on metal surfaces.

1. Introduction

The influence of defects on the pinning and sliding friction are important in many technological applications [1]. For instance, the pinning of contact lines controls the spreading of a liquid on a solid, the pinning of flux lines suppresses dissipation in type-II superconductors, and the depinning of sliding tectonic plates leads to earthquakes. Defects will also contribute to the static and kinetic friction forces during the sliding of one body on another [2].

The role of defects in the pinning and sliding of charge-density waves and of flux line systems has been studied experimentally and theoretically for many years [3, 4]. Both of these systems can, for some purposes, be considered as elastic solids interacting with defects, e.g., grain boundaries, dislocations, or point defects. Charge-density-wave systems are usually quasi-one- or two-dimensional systems (note: the charge-density-wave states tend to be more stable in low-dimensional systems as compared with 3D systems), and flux line systems in thin metal films behave as 2D solids. Thus, the influence of defects on the sliding of 1D and 2D solids is of considerable practical importance for a wide class of different systems.

It has recently been observed that adsorbate layers on metal surfaces can slide relative to the metal surface when the solid substrate performs mechanical vibrations [5]. The basic quantity deduced from the experimental data is the sliding friction $\bar{\eta}$. For a film one monolayer thick (or less) $\bar{\eta}$ determines the friction force, $-\boldsymbol{F}_0$, between the adsorbate layer and the substrate via

$$\boldsymbol{F}_0 = Nm\bar{\eta}\boldsymbol{v} \tag{1}$$

where N is the number of adsorbates and $\boldsymbol{v}$ the velocity of the adsorbate layer relative to the metal surface.

Recent experimental and theoretical studies have shown that for a compressed incommensurate Xe monolayer on Ag(111) the sliding friction $\bar{\eta}$ may be dominated by

† Permanent address: Department of Physics, Samara State Technical University, 443010 Samara, Russia.

0953-8984/97/142869+21$19.50

the direct coupling between the sliding layer and the electronic excitations in the substrate [6, 7]. Assuming that this conclusion is correct, it remains to be understood why the interaction with surface defects (e.g. steps) has a negligible influence on the sliding friction.

In this paper we study the influence of defects on the sliding friction for 1D, 2D, and 3D elastic solids. For a one-dimensional solid with a low concentration of point defects we present an exact solution, valid for arbitrary temperature and strength of the defect potential. We also discuss the role of defects (e.g. steps) on the linear (in the external driving force) sliding friction for Xe monolayers on metal surfaces.

This paper is organized as follows. In section 2 we present the model. In section 3 we calculate the leading contribution to the sliding friction at high sliding velocities. In section 4 we study the sliding friction for small-amplitude vibrations. In section 5 we present an exact solution for a 1D solid, which is valid for arbitrary temperature and strength of the defect potential. The role of defects in the linear (in the driving force) sliding friction for incommensurate Xe monolayers on metal surfaces is treated in section 6. Section 7 contains a summary and conclusions.

2. The model

We develop the model for incommensurate monolayers of Xe on silver surfaces (see also [8]). In addition to the adsorbate–substrate interaction potential $U = \sum_i u(\boldsymbol{r}_i)$ and the adsorbate–adsorbate interaction potential $V = \frac{1}{2}\sum'_{ij} v(\boldsymbol{r}_i - \boldsymbol{r}_j)$, an external force $\boldsymbol{F}$ acts on each of the adsorbates. This will lead to a drift motion such that $m\bar{\eta}\langle\dot{\boldsymbol{r}}\rangle = \boldsymbol{F}$ where $\langle\cdots\rangle$ stands for thermal averaging. For a weak external force $\boldsymbol{F}$, the sliding friction $\bar{\eta}$ is independent of $\boldsymbol{F}$.

The equation of motion for the particle coordinate $\boldsymbol{r}_i(t)$ is taken to be

$$m\ddot{\boldsymbol{r}}_i + m\eta\dot{\boldsymbol{r}}_i = -\frac{\partial U}{\partial \boldsymbol{r}_i} - \frac{\partial V}{\partial \boldsymbol{r}_i} + \boldsymbol{f}_i + \boldsymbol{F} \tag{2}$$

where $\boldsymbol{F}$ is the external force introduced above and $\boldsymbol{f}_i$ a stochastically fluctuating force which describes the influence on particle i of the irregular thermal motion of the substrate. The components f_i^α of $\boldsymbol{f}_i$ are related to the friction η via the fluctuation-dissipation theorem:

$$\langle f_i^\alpha(t) f_j^\beta(t')\rangle = 2mk_BT\eta\delta_{\alpha\beta}\delta_{ij}\delta(t-t'). \tag{3}$$

We have shown earlier [8] that for a compressed incommensurate Xe monolayer on Ag(111) the substrate corrugation is unimportant, and we therefore take U to correspond to the interaction with surface defects only. Let us write

$$U = \sum_{jn} U_d f(\boldsymbol{r}_j - \boldsymbol{R}_n) \tag{4}$$

where the $\boldsymbol{R}_n$ denote the position vectors of the defects. The strength of the defect potential is denoted by U_d and the 'form factor' by $f(\boldsymbol{x})$. For later use we will need $f(\boldsymbol{x})$ expanded in plane waves:

$$f(\boldsymbol{x}) = \int \mathrm{d}^2q \;\; f(q)\mathrm{e}^{\mathrm{i}\boldsymbol{q}\cdot\boldsymbol{x}}. \tag{5}$$

For example, if $f(\boldsymbol{x}) = \exp(-\alpha\boldsymbol{x}^2)$, then

$$f(q) = \frac{1}{4\pi\alpha}\mathrm{e}^{-q^2/4\alpha}. \tag{6}$$

Using (4) and (5) we get

$$U = U_d \sum_{jn} \int \mathrm{d}^2 q \;\; f(q) \mathrm{e}^{\mathrm{i}\boldsymbol{q}\cdot(\boldsymbol{r}_j - \boldsymbol{R}_n)}. \tag{7}$$

For Xe on silver, the microscopic friction η is mainly of electronic origin; from surface resistivity measurements and theoretical calculations $\eta \sim 3 \times 10^8$ s^{-1}.

The adsorbate–adsorbate interaction potential V is taken as a sum of Lennard-Jones pair potentials:

$$v(r) = \epsilon \left[\left(\frac{r_0}{r} \right)^{12} - 2 \left(\frac{r_0}{r} \right)^{6} \right] \tag{8}$$

where ϵ is the well depth and r_0 the particle separation at the minima in the pair potential. For Xe in the gas phase, $\epsilon = 19$ meV and $r_0 = 4.54$ Å which we also use for adsorbed Xe.

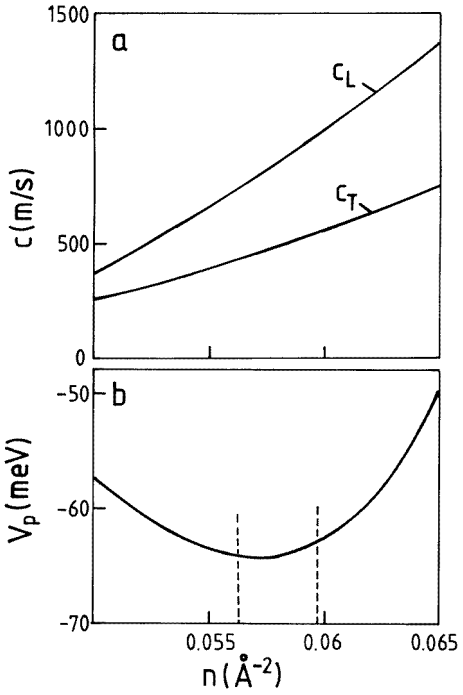

Figure 1. (a) The transverse and the longitudinal sound velocity and (b) the lateral interaction energy, as functions of the Xe coverage.

Let us now consider an adsorbate layer sliding with the velocity $\boldsymbol{v}$ on a substrate. Let us write the coordinates for the particles in the sliding state as

$$\boldsymbol{r}_i = \boldsymbol{v}t + \boldsymbol{x}_i + \boldsymbol{u}_i \tag{9}$$

where $\boldsymbol{v}$ is the drift velocity, the $\boldsymbol{x}_i = (x_i, y_i)$ are the perfect-lattice sites (in a reference frame moving with the velocity $\boldsymbol{v}$) of the hexagonal structure, and the $\boldsymbol{u}_i$ are the (fluctuating) displacements away from these sites. Substituting (9) in the equation of motion (2) and expanding V to linear order in $\boldsymbol{u}_i$ gives

$$m\ddot{\boldsymbol{u}}_i + m\eta\dot{\boldsymbol{u}}_i + \sum_j K_{ij}\boldsymbol{u}_j = \boldsymbol{f}_i + \boldsymbol{F} - m\eta\boldsymbol{v} - \frac{\partial U}{\partial \boldsymbol{x}_i}(\boldsymbol{x}_i + \boldsymbol{v}t + \boldsymbol{u}_i) \tag{10}$$

where the force constant matrix K_{ij} has the components $K_{ij}^{\alpha\beta} = \partial^2 V/\partial u_i^\alpha\, \partial u_j^\beta$. Let us introduce the matrix $K(\boldsymbol{q})$ with the components

$$K^{\alpha\beta}(\boldsymbol{q}) = \sum_j K_{ij}^{\alpha\beta} \mathrm{e}^{-\mathrm{i}\boldsymbol{q}\cdot(\boldsymbol{x}_i - \boldsymbol{x}_j)}$$

or

$$K^{\alpha\beta}(\boldsymbol{q}) = \frac{6\epsilon}{r_0^2} \sum_{n\neq 0} \left[(\xi_n^4 - \xi_n^7)\delta_{\alpha\beta} + (14\xi_n^8 - 8\xi_n^5)\frac{x_n^\alpha x_n^\beta}{r_0^2} \right] (1 - \mathrm{e}^{\mathrm{i}\boldsymbol{q}\cdot\boldsymbol{x}_n}) \tag{11}$$

where $\xi_n = r_0^2/\boldsymbol{x}_n^2$ and where the sum is over all of the sites $\boldsymbol{x}_n$ of the hexagonal lattice of the adsorbate layer (excluding the site at the origin). In the limit $q \to 0$ we can expand (11) to quadratic order in $\boldsymbol{q}$ to get

$$K^{\alpha\beta} = mc_T^2 q^2 \delta_{\alpha\beta} + m(c_L^2 - c_T^2) q_\alpha q_\beta. \tag{12}$$

In figure 1(a) we show the transverse (c_T) and the longitudinal (c_L) sound velocities as functions of the Xe coverage. Figure 1(b) shows (for $U = 0$) the Xe–Xe interaction potential, $V_p = \sum_j' v_{0j}/2$, as a function of coverage. All of the quantities refer, of course, to zero temperature. The two vertical dashed lines correspond to the coverage of the uncompressed Xe monolayer film ($n_a = 0.056\,24$ Å^{-2}) and the compressed film (0.0597 Å^{-2}) at the temperature $T = 77.4$ K.

For steady sliding at small velocities v, only vibrations with large wavelength $\lambda \sim (c/v)a$, where a is the lattice constant and c is the sound velocity, can be excited in the adsorbed film. If $\lambda \gg a$ (i.e. $v \ll c$), one can neglect the discrete nature of the film and use the elastic continuum model. If the thickness of the film $h \ll \lambda$, only vibrations with the wave vector parallel to the surface can be excited. Because of this, for $\lambda \gg a, h$, the adsorbate film can be considered as an elastic plate. In the plate it is possible to excite bending vibrations, and also elastic waves with the wave vector parallel to the plate, which are uniform over the thickness of the plate. However, due to the interaction with the substrate, the bending vibrations have frequencies which are much higher than the washboard frequency v/a, and will not contribute to the sliding friction.

Let us derive the (long-wavelength) continuum limit of (10). In the continuum limit $\boldsymbol{u}_i(t) \to \boldsymbol{u}(\boldsymbol{x}, t)$, and using (12) the left-hand side of (10) takes the form

$$m\left(\frac{\partial^2 \boldsymbol{u}}{\partial t^2} + \eta \frac{\partial \boldsymbol{u}}{\partial t} - c_T^2 \nabla^2 \boldsymbol{u} - (c_L^2 - c_T^2)\boldsymbol{\nabla}\boldsymbol{\nabla}\cdot\boldsymbol{u} \right).$$

The fluctuating force $\boldsymbol{f}_i(t) \to \boldsymbol{f}(\boldsymbol{x}, t)/n_a$ where $\boldsymbol{f}$ is the fluctuating force per unit area (n_a is the number of adsorbates per unit area). The continuum limit of (3) is

$$\langle f_\alpha(\boldsymbol{x}, t) f_\beta(\boldsymbol{x}', t')\rangle = 2\rho k_B T \eta \delta_{\alpha\beta}\delta(\boldsymbol{x} - \boldsymbol{x}')\delta(t - t') \tag{13}$$

where $\rho = mn_a$. Finally, note that in the continuum limit the potential

$$U \to \sum_{jn} U_d f(\boldsymbol{x}_j + \boldsymbol{v}t + \boldsymbol{u}(\boldsymbol{R}_n, t) - \boldsymbol{R}_n) = n_a U_d (2\pi)^2 \sum_{n\boldsymbol{G}} f(G) \mathrm{e}^{\mathrm{i}\boldsymbol{G}\cdot[\boldsymbol{v}t + \boldsymbol{u}(\boldsymbol{R}_n, t) - \boldsymbol{R}_n]}.$$

In the simplest case one includes only the contribution from the smallest reciprocal-lattice vectors $\{\boldsymbol{G}\}$ in this expansion. Thus, for example, in the 1D case, which we consider in detail below,

$$U = \text{constant} + 2U_d k f(k) \sum_n \cos(k[vt + u(R_n, t) - R_n]) \tag{14}$$

where $k = 2\pi/a$, and a is the lattice constant. Multiplying (2) by $n_a = 1/a$ gives in the 1D case the continuum equation

$$\rho\left(\frac{\partial^2 u}{\partial t^2} + \eta\frac{\partial u}{\partial t} - c^2\frac{\partial^2 u}{\partial x^2}\right) = f(x,t) + n_a F - \rho\eta v - \lambda\sum_n \sin(k[vt + u(R_n,t) - R_n])\delta(x - R_n) \tag{15}$$

where

$$\lambda = 2U_d k^2 f(k). \tag{16}$$

3. High sliding velocities

Let us calculate the leading contribution to the sliding friction for high sliding velocities and zero temperature. When the sliding velocity v is very high, the particles have no time to adjust to the rapidly fluctuating forces from the pinning centres—hence the particle trajectories will be nearly straight lines. Due to the particle–particle interactions the system will therefore form a nearly perfect hexagonal structure as expected in the absence of pinning centres. Now, as v decreases the particles will, in response to the forces from the pinning centres, oscillate with increasing amplitude around the perfect-lattice sites. The treatment presented below is only valid as long as the displacement of the atoms away from the lattice sites is small compared to the lattice constant.

For large v, $|\boldsymbol{u}_i|$ is small. Substituting (7) in (10) and expanding to linear order in $\boldsymbol{u}_i$ gives

$$m\ddot{\boldsymbol{u}}_i + m\eta\dot{\boldsymbol{u}}_i + \sum_j K_{ij}\boldsymbol{u}_j = m(\bar{\eta} - \eta)\boldsymbol{v} - U_d\int \mathrm{d}^2q\ G(\boldsymbol{q})f(q)\mathrm{i}\boldsymbol{q}\mathrm{e}^{\mathrm{i}\boldsymbol{q}\cdot(\boldsymbol{x}_i + \boldsymbol{v}t)} + U_d\int \mathrm{d}^2q\ G(\boldsymbol{q})f(q)\boldsymbol{q}\boldsymbol{q}\cdot\boldsymbol{u}_i\mathrm{e}^{\mathrm{i}\boldsymbol{q}\cdot(\boldsymbol{x}_i+\boldsymbol{v}t)} \tag{17}$$

where

$$G = \sum_m \mathrm{e}^{-\mathrm{i}\boldsymbol{q}\cdot\boldsymbol{R}_m}.$$

Let $\langle\cdots\rangle$ stand for time averaging and for averaging over the random distributions of impurity centres. We have $\langle G\rangle = 0$ and

$$\langle G(\boldsymbol{q})G(\boldsymbol{q}')\rangle = N_d\delta_{\boldsymbol{q}+\boldsymbol{q}',\boldsymbol{0}} \to (2\pi)^2 n_d\delta(\boldsymbol{q} + \boldsymbol{q}') \tag{18}$$

where N_d and n_d are the total number of defects and the number of defects per unit area, respectively. Since furthermore $\langle\boldsymbol{u}_i\rangle = 0$, we get from (17)

$$\boldsymbol{0} = m(\bar{\eta} - \eta)\boldsymbol{v} - U_d\int \mathrm{d}^2q\ f(q)\boldsymbol{q}\boldsymbol{q}\cdot\langle G(\boldsymbol{q})\boldsymbol{u}_i\rangle\mathrm{e}^{\mathrm{i}\boldsymbol{q}\cdot(\boldsymbol{x}_i+\boldsymbol{v}t)}. \tag{19}$$

To linear order in U_d we obtain from (17)

$$\boldsymbol{u}_i = -\frac{\mathrm{i}U_d}{m}\int \mathrm{d}^2q\ \frac{G(\boldsymbol{q})f(q)\mathrm{e}^{\mathrm{i}\boldsymbol{q}\cdot(\boldsymbol{x}_i+\boldsymbol{v}t)}}{(\boldsymbol{q}\cdot\boldsymbol{v})^2 + \mathrm{i}\eta\boldsymbol{q}\cdot\boldsymbol{v} - \omega^2(\boldsymbol{q})}\boldsymbol{q} \tag{20a}$$

where $\omega^2(\boldsymbol{q})$ is a matrix with the components $K^{\alpha\beta}/m$, which, in the long-wavelength limit, takes the form (see (12))

$$c_T^2 q^2\delta_{\alpha\beta} + (c_L^2 - c_T^2)q_\alpha q_\beta.$$

Let $\boldsymbol{e}_s(\boldsymbol{q})$ denote the eigenvectors of the matrix $\omega^2(\boldsymbol{q})$, corresponding to the eigenvalues $\omega_s^2(\boldsymbol{q})$. Expanding $\boldsymbol{q} = \sum_s \boldsymbol{q}\cdot\boldsymbol{e}_s\boldsymbol{e}_s$ and substituting in (20*a*) gives

$$\boldsymbol{u}_i = -\frac{\mathrm{i}U_d}{m}\sum_s \int \mathrm{d}^2q\ \frac{G(\boldsymbol{q})f(q)\mathrm{e}^{\mathrm{i}\boldsymbol{q}\cdot(\boldsymbol{x}_i+\boldsymbol{v}t)}}{(\boldsymbol{q}\cdot\boldsymbol{v})^2 + \mathrm{i}\eta\boldsymbol{q}\cdot\boldsymbol{v} - \omega_s^2(\boldsymbol{q})}\boldsymbol{q}\cdot\boldsymbol{e}_s\boldsymbol{e}_s. \tag{20b}$$

Using (18) and (20*b*) gives

$$\langle \boldsymbol{u}^2\rangle = \frac{(2\pi)^2U_d^2n_d}{m^2}\sum_s\int \mathrm{d}^2q\ \frac{(\boldsymbol{q}\cdot\boldsymbol{e}_s)^2|f(q)|^2}{[(\boldsymbol{q}\cdot\boldsymbol{v})^2-\omega_s^2(\boldsymbol{q})]^2 + (\eta\boldsymbol{q}\cdot\boldsymbol{v})^2}. \tag{21}$$

Substituting (20*b*) in (19), using (18), and assuming $\boldsymbol{v} = \hat{\boldsymbol{x}}v$ gives after some simplifications

$$\bar{\eta} = \eta + \frac{(2\pi)^2U_d^2n_d}{m^2}\sum_s\int \mathrm{d}^2q\ \frac{\eta q_x^2(\boldsymbol{q}\cdot\boldsymbol{e}_s)^2|f(q)|^2}{[q_x^2v^2-\omega_s^2(\boldsymbol{q})]^2 + \eta^2q_x^2v^2}. \tag{22}$$

Since η is 'small' we can take the limit $\eta\to 0$ when evaluating the integral in (22). Using

$$\frac{\Gamma}{x^2+\Gamma^2} \to \pi\delta(x) \qquad \text{as } \Gamma\to 0$$

we get

$$\bar{\eta} = \eta + \frac{(2\pi)^2U_d^2n_d}{m^2v}\sum_s\int \mathrm{d}^2q\ |q_x|(\boldsymbol{q}\cdot\boldsymbol{e}_s)^2|f(q)|^2\pi\delta[q_x^2v^2-\omega_s^2(\boldsymbol{q})].$$

Now, note that $\omega_s(\boldsymbol{q}+\boldsymbol{G}) = \omega_s(\boldsymbol{q})$. We assume $v \ll c_L, c_T$, and the contributions to the integral in (22) will then occur only for $\boldsymbol{q}\approx\boldsymbol{G}$ with $G_x \neq 0$. We get

$$\bar{\eta} = \eta + \frac{(2\pi^2)^2U_d^2n_d}{m^2v}\sum_{s\boldsymbol{G}}{}' |G_x|(\boldsymbol{G}\cdot\boldsymbol{e}_s)^2|f(G)|^2/c_s^2 \tag{23}$$

where the prime on the summation symbol indicates that in the sum over $\boldsymbol{G}$, the reciprocal-lattice vectors with $G_x = 0$ are excluded. Similarly using (21) we get

$$\langle \boldsymbol{u}^2\rangle = \frac{(2\pi^2)^2U_d^2n_d}{m^2\eta v}\sum_{s\boldsymbol{G}}{}' \left[(\boldsymbol{G}\cdot\boldsymbol{e}_s)^2/|G_x|\right]|f(G)|^2/c_s^2. \tag{24}$$

In a similar way one obtains for a 1D solid

$$\bar{\eta} = \eta + \frac{2\pi^2U_d^2n_d}{m^2cv^2}\sum_G{}' G^2|f(G)|^2 \tag{25}$$

and

$$\langle u^2\rangle = \frac{2\pi^2U_d^2n_d}{m^2\eta cv^2}\sum_G{}' (G^2/G_x^2)|f(G)|^2 \tag{26}$$

and for a 3D solid

$$\bar{\eta} = \eta + \frac{(2\pi)^5U_d^2n_d}{2m^2}\sum_{s\boldsymbol{G}}{}' G_x^2(\boldsymbol{G}\cdot\boldsymbol{e}_s)^2|f(G)|^2/c_s^3 \tag{27}$$

and

$$\langle \boldsymbol{u}^2\rangle = \frac{(2\pi)^5U_d^2n_d}{2m^2\eta}\sum_{s\boldsymbol{G}}{}' (\boldsymbol{G}\cdot\boldsymbol{e}_s)^2|f(G)|^2/c_s^3. \tag{28}$$

The most important result obtained above is the velocity dependence of $\bar{\eta}-\eta$ and of $\langle u^2\rangle$ which we summarize as follows:

1D: $\sim 1/v^2$ 2D: $\sim 1/v$ 3D: ~ 1.

Now, the expansion of U in $\boldsymbol{u}_i$, on which the derivation of (23)–(28) is based, is only valid if $\langle \boldsymbol{u}^2 \rangle \ll a^2$ where a is the lattice constant. Hence it is clear that in the 3D case, if U_d is small enough or η large enough, since $\langle u^2 \rangle$ is independent of v the results (27) and (28) are *valid for all sliding velocities*, and the friction force $F_0 = m\bar{\eta}v \sim v$ for all v (but $v \ll c$). (This statement is actually not quite true: in the calculation above we have neglected the modifications in the adsorbate–substrate interaction due to the motion of the substrate atoms. This is an excellent approximation at high sliding velocity but breaks down at low sliding velocity. An analysis shows that at very low sliding velocity the friction force is again proportional to the velocity but the proportionality factor is different to that in the high-velocity region due to (adiabatic) renormalization of the adsorbate–substrate coupling; see the next section.) However, for the 1D and 2D systems, $\langle u^2 \rangle$ diverges as $v \to 0$, and it is clear that *independently of how weak the defect potential U_d is, at low enough velocities v the expansion on which (23)–(26) are based will break down*. Physically, this difference between 3D systems and 1D and 2D systems is related to the 'softness' of the elastic properties of low-dimensional solids: in 1D and 2D solids a force applied at some point in the solid gives rise to an infinitely large elastic displacement (for a finite system, of linear size L, the elastic displacement scales as $u \sim L$ and $\sim \ln L$ for 1D and 2D solids, respectively). A similar conclusion has been reached by Sokoloff [9].

The condition given above for the validity of the high-velocity expansion, namely that $\langle u^2 \rangle \ll a^2$, is the correct one only if the defect concentration n_d is large enough. The point is that $\langle u^2 \rangle$ is the *average* over all of the atoms in the sliding lattice, while the condition for the validity of the high-velocity expansion is that the displacement u_i of *all* of the atoms in the lattice must be small compared to the lattice constant a. Since the displacement u_i of an atom which is (temporarily) close to a defect is likely to be larger than for an atom far away, it is clear that the condition $\langle u^2 \rangle \ll a^2$ may not always guarantee the validity of the high-v expansion. To illustrate this, let us first consider the 1D case. For a single defect it is easy to show from the 1D version of (20*b*) that the maximum displacement u_i of an atom when it is close to a defect is given by

$$u_{max} = U_d \frac{\pi}{2mcv} \sum_G f(G).$$

Thus $\langle u^2 \rangle \sim u_{max}^2$ gives $n_d \sim \eta/4c$, so for $n_d > \eta/4c$ the condition $\langle u^2 \rangle \ll a^2$ guarantees that the high-v expansion holds. Similarly, for a 2D system one can show that if the defect concentration $n_d > 4\pi\eta v/c^2 a$, then the condition $\langle u^2 \rangle \gg a^2$ will guarantee the validity of the high-velocity expansion. For Xe on a silver surface $\eta \sim 3 \times 10^8$ s^{-1}, the sound velocity $c \sim 500$ s^{-1} and, with the typical sliding velocity $v \sim 1$ cm s^{-1}, the inequality above reduces to $n_a > 10^{-8}$ Å^{-2}, which is usually satisfied in quartz crystal microbalance friction measurements.

4. Small-amplitude vibrations

Another limiting case which can be solved exactly is that of the friction associated with small-amplitude vibrations. We assume again a low concentration of randomly distributed defects. In this case the defects will contribute independently of each other, and it is enough to calculate the friction force associated with a single defect. This is most conveniently done as follows. Let ξ denote the coordinate of a defect (we consider first the 1D case so that ξ is a scalar); see figure 2. Assume that the defect is connected to the 1D elastic solid at the point $x = 0$ via a spring with force constant K which is determined by expanding $U(\boldsymbol{x})$ to second order in $\boldsymbol{x}$. We assume that the defect performs vibrations relative to the elastic

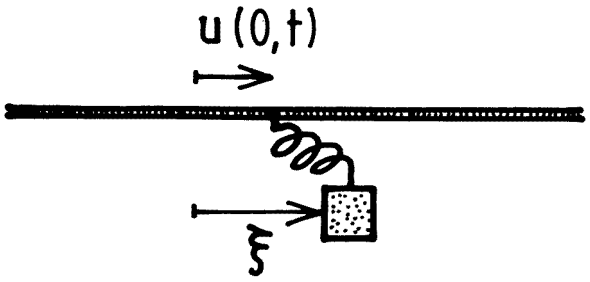

Figure 2. A defect connected to a 1D elastic solid via a spring (spring constant K).

solid, and calculate the force acting on the defect from the solid. This force should be the same as the force acting on a stationary defect if the elastic solid performs translational vibrations (with the same amplitude and frequency) relative to the defects.

The force on the defect from the elastic media

$$F_0(t) = -K[\xi - u(0,t)].$$

The defect particle exerts a force $K[\xi - u(0,t)]$ on the elastic media at the point $x = 0$, so the equation of motion of the elastic media becomes

$$\rho\left(\frac{\partial^2 u}{\partial t^2} + \eta\frac{\partial u}{\partial t} - c^2\frac{\partial^2 u}{\partial x^2}\right) = K[\xi - u(0,t)]\delta(x). \tag{29}$$

This equation is easy to solve:

$$u(0,\omega) = K[\xi(\omega) - u(0,\omega)]\frac{1}{2\pi}\int \mathrm{d}q\ \frac{1}{\rho(-\omega^2 - \mathrm{i}\eta\omega + c^2q^2)} = A[\xi(\omega) - u(0,\omega)] \tag{30}$$

where, in the limit $\eta \to 0$,

$$A = \mathrm{i}K/2c\rho\omega.$$

It is easy to solve (30) for $u(0,\omega)$:

$$u(0,\omega) = \frac{A\xi(\omega)}{1+A}$$

so the force F_0 acting on the defect

$$F_0(\omega) = -K[\xi(\omega) - u(0,\omega)] = -\frac{K\xi(\omega)}{1+A} \to \mathrm{i}\omega\xi\, 2\rho c \tag{31}$$

as $\omega \to 0$. Thus

$$F(t) = -2\rho c\dot{\xi}. \tag{32}$$

It is remarkable that the force F which acts on the defect is *independent* of the original coupling strength (spring constant K) and that it is purely dissipative. That is, no *elastic* restoring force occurs for a 1D solid. The physical origin of this is related to the fact that an arbitrary weak force applied to a point of a 1D elastic solid gives rise to an infinite displacement (for a finite 1D solid the displacement is proportional to the linear size L of the solid). The physical origin of the friction force, $-2\rho c\dot{\xi}$, will be discussed in section 4. If we have N_d defects, the total friction force $N_d 2\rho cv = Nm\bar{\eta}v$, or

$$\bar{\eta} = \eta + 2n_d c \tag{33}$$

where we have added the contribution η from the direct coupling to the substrate and where we have used the fact that $N_d\rho/Nm = n_d$.

In a similar way to the above, it is easy to calculate the friction force for small-amplitude vibrations for 2D and 3D solids, and here we only quote the results for low frequencies. For a 3D system

$$A = \frac{K}{2\pi^2\rho c_T^2}\int_0^{q_c} \mathrm{d}q\ \frac{q^2}{q^2-\omega^2/c_T^2-\mathrm{i}0^+}\left(1+\frac{q^2(c_T^2/c_L^2-1)/3}{q^2-\omega^2/c_L^2-\mathrm{i}0^+}\right)$$
$$= B(\omega)+\mathrm{i}\frac{K\omega}{6\pi\rho c_T^3}\left[1+\frac{1}{2}\left(\frac{c_T}{c_L}\right)^3\right] \tag{34}$$

where the real part $\mathrm{Re}\,A = B(\omega) \to$ constant as $\omega \to 0$. Thus

$$F_0(\omega) = -\bar{K}\xi - \frac{\bar{K}^2}{6\pi\rho c_T^3}\left[1+\frac{1}{2}\left(\frac{c_T}{c_L}\right)^3\right]\dot{\xi} = 0 \tag{35}$$

where the renormalized spring constant $\bar{K} = K/[1-B(0)]$. We note that a very similar expression for the friction force has been derived in reference [10] for adsorbates performing parallel or perpendicular vibrations on surfaces of semi-infinite solids.

For a 2D system

$$A = \frac{K}{2\pi\rho c_T^2}\int_0^{q_c} \mathrm{d}q\ \frac{q}{q^2-\omega^2/c_T^2-\mathrm{i}0^+}\left(1+\frac{q^2(c_T^2/c_L^2-1)/2}{q^2-\omega^2/c_L^2-\mathrm{i}0^+}\right)$$
$$= \frac{K}{4\pi\rho c_T^2}\left[\ln\left(\frac{q_c c_T^2}{\omega c_L}\right)+\frac{c_T^2}{c_L^2}\ln\left(\frac{q_c c_T}{\omega}\right)\right]+\mathrm{i}\frac{K}{8\rho c_T^2}\left(1+\frac{c_T^2}{c_L^2}\right). \tag{36}$$

Note that the real term in this expression diverges logarithmically when $\omega \to 0$. This implies that the elastic restoring force vanishes as $\omega \to 0$. The physical origin of this is again the 'softness' of 2D elastic solids, where the displacement of a point P, in response to a weak force applied at P, diverges logarithmically with the linear size L of the solid. However, the logarithmic divergence in (36) is of no practical importance because any real measurement involves finite frequencies ω (the external force has to be turned on and turned off, and immediately this generates finite frequencies), and also because any real system has a finite size L which implies that the q-integral in (36) must be cut-off at $q_{min} \sim 1/L$, rather than extended right down to zero, and this removes the $\omega \to 0$ divergence of (36). Thus, for a 2D solid the small-amplitude friction force has the form

$$F_0(\omega) = -K\xi/(1+A) = -(K_1+\mathrm{i}K_2)\xi \tag{37}$$

where both the real part (elastic spring constant) K_1 and the imaginary part K_2 are finite as $\omega \to 0$.

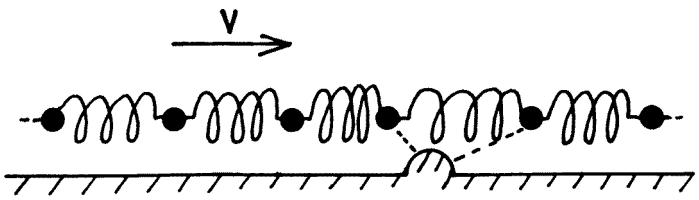

Figure 3. An elastic string sliding on a flat 'substrate' with a point imperfection.

5. Exact solution for a 1D solid

In this section we present an exact solution to (15) for one defect (see figure 3), valid for arbitrary temperature and defect strength [11]. The basic equation is

$$\rho\left(\frac{\partial^2 u}{\partial t^2}+\eta\frac{\partial u}{\partial t}-c^2\frac{\partial^2 u}{\partial x^2}\right)=f(x,t)+n_aF-\rho\eta v-\lambda\sin[k(vt+u)]\delta(x) \tag{38}$$

where

$$\lambda=2U_dk^2f(k). \tag{39}$$

The fluctuating force $f(x,t)$ satisfies (13):

$$\langle f(x,t)f(x',t')\rangle=2\rho k_BT\eta\delta(x-x')\delta(t-t'). \tag{40}$$

Let us write

$$f(x,t)=\frac{1}{(2\pi)^2}\int \mathrm{d}q\ \mathrm{d}\omega\ f(q,\omega)\mathrm{e}^{\mathrm{i}(qx-\omega t)}. \tag{41}$$

Substituting (41) in (40) gives

$$\langle f(q,\omega)f(q',\omega')\rangle=2\rho k_BT\eta(2\pi)^2\delta(q+q')\delta(\omega+\omega'). \tag{42}$$

A single impurity in an infinite system cannot affect the sliding friction *per particle*, so $F=m\bar{\eta}v=m\eta v$. Thus $v=F/m\eta$, and the term $n_aF-\rho\eta v$, which occurs in (38), vanishes. The solution to (38) for $x=0$ can be written as

$$u(0,t)=u_T(0,t)+\int_{-\infty}^{t}\mathrm{d}t'\ G(t-t')\lambda\sin k[vt'+u(0,t')] \tag{43}$$

where

$$G(t)=\frac{1}{2\pi\rho c}\int_0^1\mathrm{d}s\ \frac{\mathrm{e}^{-\eta ts}}{(s-s^2)^{1/2}} \tag{44}$$

and where u_T is the contribution to u from the fluctuating force $f(x,t)$:

$$u_T(0,t)=\frac{1}{(2\pi)^2}\int \mathrm{d}q\ \mathrm{d}\omega\ \frac{f(q,\omega)\mathrm{e}^{-\mathrm{i}\omega t}}{\rho(c^2q^2-\omega^2-\mathrm{i}\omega\eta)}. \tag{45}$$

Let us take the time derivative of (43). We get, with $u(0,t)=u(t)$,

$$\frac{\mathrm{d}u}{\mathrm{d}t}=\frac{\mathrm{d}u_T}{\mathrm{d}t}+\lambda G(0)\sin k[vt+u(t)]-\eta\int_{-\infty}^{t}\mathrm{d}t'\ H(t-t')\lambda\sin k[vt'+u(t')] \tag{46}$$

where

$$H(t)=\frac{1}{2\pi\rho c}\int_0^1\mathrm{d}s\ \frac{s\mathrm{e}^{-\eta ts}}{(s-s^2)^{1/2}}. \tag{47}$$

It is easy to calculate

$$G(0)=1/2\rho c\qquad H(0)=1/4\rho c. \tag{48}$$

Note that

$$\langle\dot{u}_T(t)\dot{u}_T(0)\rangle=\frac{1}{(2\pi)^4}\int \mathrm{d}q\ \mathrm{d}q'\ \mathrm{d}\omega\ \mathrm{d}\omega'\ (-\omega\omega')\mathrm{e}^{-\mathrm{i}\omega t}$$
$$\times\ \frac{2\rho\eta k_BT(2\pi)^2\delta(\omega+\omega')\delta(q+q')}{\rho^2(c^2q^2-\omega^2-\mathrm{i}\omega\eta)(c^2q'^2-\omega'^2-\mathrm{i}\omega'\eta)}=\frac{k_BT}{\rho c}\delta(t). \tag{49}$$

We assume that η is 'small' and calculate the contribution from the defect to the friction force to first order in η.

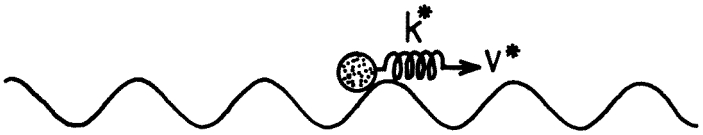

Figure 4. The sliding friction dynamics when a 1D elastic solid slides over a defect is equivalent to a particle moving in a periodic potential and being pulled by a harmonic spring.

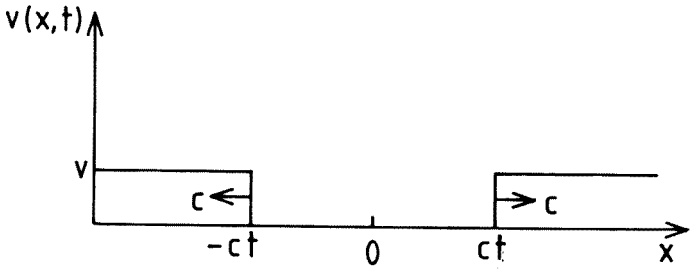

Figure 5. In the limit $\eta \to 0$ and for $v < U_d k^2 f(k)/\rho c$ the solid is pinned at the defect and the 'friction' is due to the 'stopping wave' emitted from the defect, propagating to the right and to the left with the sound velocity c.

To first order in η we can put $\eta = 0$ in the integral $H(t)$. Using $H(0) = 1/4\rho c$ this gives

$$\frac{\mathrm{d}u}{\mathrm{d}t} = \frac{\mathrm{d}u_T}{\mathrm{d}t} + (\lambda/2\rho c)\sin k[vt + u(t)] - \eta(\lambda/4\rho c)\int_{-\infty}^{t} \mathrm{d}t' \ \sin k[vt' + u(t')]. \tag{50}$$

Now, note that to zero order in η equation (43) gives

$$(\lambda/2\rho c)\int_{-\infty}^{t} \mathrm{d}t' \ \sin k[vt' + u(t')] = u - u_T. \tag{51}$$

Substituting this in (50) gives to first order in η

$$\frac{\mathrm{d}u}{\mathrm{d}t} = \frac{\mathrm{d}u_T}{\mathrm{d}t} + (\lambda/2\rho c)\sin k[vt + u(t)] - (\eta/2)(u - u_T). \tag{52}$$

We introduce $X = k(vt + u)$, $F^* = kv$, $f^* = k\dot{u}_T$, and $U_d^* = k\lambda/2\rho c$, so

$$\frac{\mathrm{d}X}{\mathrm{d}t} = F^* + f^* + k\eta u_T + (\eta/2)(kvt - X) + U_d^* \sin X \tag{53}$$

where

$$\langle f^*(t) f^*(0)\rangle = 2T^*\delta(t)$$
$$T^* = \frac{k_B T}{\rho c}k^2.$$

In (53) $k\eta u_T$ gives a small contribution to the fluctuating force f^* which has no important physical effects and we neglect this term. If we interpret $\eta/2 = k^*$ as a spring constant, then (53) takes the form

$$\frac{\mathrm{d}X}{\mathrm{d}t} = f^* + k^*(v^*t + X_0 - X) + U_d^* \sin X \tag{54}$$

where

$$X_0 = F^*/k^* \qquad k^* = \eta/2 \qquad v^* = kv. \tag{55}$$

Equation (54) describes a particle connected to a spring (spring constant k^*) where the free end of the spring moves with the velocity v^*. The particle moves in the potential $U^* = U_d^* \cos X$ and under the influence of the fluctuating force f^*; see figure 4. Since the force from the spring in (54) increases linearly with time, after a long enough time the spring force will be large enough to overcome the pinning barrier. Note that the contribution $k^*(v^*t + X_0)$ to the spring force in the original quantities takes the form

$$(F/2)(2ct/a) + 2\rho cv. \tag{56}$$

To understand this expression, consider an elastic string which slides (velocity v) on a surface (along the x-axis) with one defect at $x = 0$. Assume that at time $t = 0$, the string atoms at the defects get pinned. This will generate a *stopping wave* which propagates to the right and to the left with the sound velocity c; see figure 5. To zero order in η the displacement field $u(x, t)$ is easy to calculate. For example, for $x > 0$,

$$u_0 = vt \qquad \text{for } x > ct$$
$$u_0 = vx/c \qquad \text{for } x < ct$$

or

$$u_0 = vt + (v/c)(x - ct)\theta(ct - x). \tag{57}$$

Thus the force on the defect, from the stopping wave occurring to the right of the defect, is $\rho c^2\, \partial u/\partial x(0, t) = \rho cv$. Similarly the force from the stopping wave from the region to the left of the defect equals ρcv. Thus the total force equals $2\rho cv$ which gives the zero-order (in η) term in (56). Note that if the force from the stopping waves is bigger than the force $\lambda = 2U_d k^2 f(k)$ necessary to overcome the defect barrier, no pinning or local stick–slip will occur. Thus to zero order in η, steady sliding occurs if $2\rho cv > 2U_d k^2 f(k)$ or $v > U_d k^2 f(k)/\rho c$. For a detailed discussion of the $\eta = 0$ limit, see appendix A.

The first term in (56) is of first order in η and has the following physical origin. On the moving atoms for $x > ct$ (and $x < -ct$), the driving force F and the friction force $m\eta v$ act, and since the atoms do not accelerate these forces are equal. Now, on the 'stopped' atoms, for $-ct < x < ct$, the latter force vanishes, but the external force F still acts, and must in equilibrium be balanced by the spring forces between the particles. Since the number of 'stopped' atoms at time t equals $2ct/a$, the total force (derived from the external force F) acting on the defect equals $(F/2)(2ct/a)$. The origin of the factor of $F/2$—rather than F—lies in the fact that when the stopping wave arrives at $x = ct$, it takes a time $t = x/c$ for that 'message' to propagate back to the defect. Thus, effectively, only the external force acting on half of the atoms contained in the 'stopped' region will contribute to the force acting on the defect.

Let us discuss the origin of the first term in (56) in detail. We calculate the displacement field u to first order in η. The zero-order solution (in η) u is given by (57). Now, let us write $u = u_0 + u_1$ and require that, to linear order in η, u satisfies the equation of motion

$$\rho\left(\frac{\partial^2 u}{\partial t^2} + \eta\frac{\partial u}{\partial t} - c^2\frac{\partial^2 u}{\partial x^2}\right) = n_a F \tag{58}$$

and the boundary conditions $u(0, t) = 0$ and $u(ct, t) = vt$. This gives

$$u_1 = (\eta v/2c^2)x(ct - x)\theta(ct - x). \tag{59}$$

The force which acts on the defect from the elastic solid to the right of it is given by

$$\rho c^2 \, \partial u/\partial x(0,t) = \rho c v + (F/2)(ct/a) \tag{60}$$

where $F = m\eta v$. The force from the elastic solid to the left of the defect is also given by (60). Thus the total force is the same as obtained above (see (56)).

Let us discuss the nature of the solutions of (54). For high sliding velocity we can write

$$X = v^* t + \xi \tag{61}$$

where ξ is small. Substituting this in (54) gives to leading order in $1/v^*$

$$\xi = -(U_d^*/v^*) \cos v^* t. \tag{62}$$

The force on the defect is

$$F_0 = -\lambda \langle \sin X \rangle = -\lambda \langle \sin(v^* t + \xi) \rangle \approx -\lambda \langle \sin v^* t + \xi \cos v^* t \rangle. \tag{63}$$

Substituting (62) in (63) and performing the time average gives the kinetic friction force

$$F_0 = \lambda U_d^*/2v^*. \tag{64}$$

Substituting (39) in this expression gives the same high-velocity result as was derived earlier (see (25) with $G = \pm 2\pi/a$ included in the sum). It is clear that for very large v the velocity of the solid at the defect has only a small modulation $\sim \cos(kvt)$ around the steady drift velocity v occurring far away from the defect. Associated with these periodic oscillations will be a damping caused by emission of sound waves. We note that the derivation of (64) requires $|\xi| \ll 1$ or, using (62), $U_d^*/v^* \ll 1$, which is identical to the condition for the high-velocity expansion for a single-impurity case derived at the end of section 4.

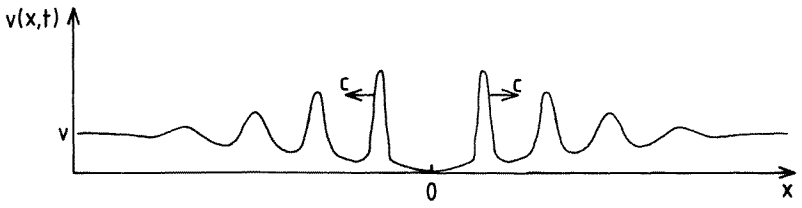

Figure 6. At low driving force F the solid at the defect will perform stick–slip motion. This results in a series of wave pulses being emitted from the defect, propagating both to the right and to the left of the defect with the sound velocity c. Because of the finite friction η, the wave pulses are damped (the damping and the width of the wave pulses are exaggerated).

Let us now consider very low sliding velocities. Assume first zero temperature. We must consider two different cases. If the spring k^* is weak or the amplitude U_d^* of the defect potential high, an elastic instability occurs and the motion of the particle will always be rapid during some time periods of the sliding, independently of how low the driving velocity v^* is. On the other hand if the spring is stiff or U_d^* small, no elastic instability will occur and the velocity $\dot{X}$ of the particle will always be of order v^*. For a cosine potential, $U^* = U_d^* \cos X$, the elastic instability will occur if $U_d^* > k^*$ or

$$k\lambda > \rho c \eta. \tag{65}$$

In most cases of interest this inequality is satisfied. In such cases the elastic solid at the defect will perform stick–slip motion, where (for small v^*) 'long' stick-time periods are interrupted by rapid slipping. During sticking the spring force increases continuously with increasing time, while X is nearly constant, until the critical force necessary to overcome

the pinning barrier is reached, at which point rapid slipping starts. This will result in a series of wave pulses being emitted from the defects. In each pulse the solid moves with a high velocity, but because of the damping η the 'height' of the pulses decreases, so far away from the defect the displacement field asymptotically approaches $u = vt$; see figure 6. Since the motion is overdamped the 'particle' relaxes down in the next potential well in the periodic potential $U_d^* \cos X$, i.e. the *elastic solid in each stick–slip cycle is displaced by a single lattice constant*. The physical origin of the overdamped motion is the emission of sound waves during the rapid local slipping. If we define the kinetic friction force as the force on the defect averaged over time, it is enough to include the stick-time period in the average, as the slipping occurs very quickly on the time-scale of a complete stick–slip period. During a sticking period the spring force increases (approximately) linearly with time. If the sliding velocity is v, the time of a stick–slip period is a/v. The spring force at the onset of slipping is approximately λ. During slipping, v^*t is nearly constant, while X increases by 2π, corresponding to a displacement by one lattice constant. Thus, during slipping, the spring force decreases to $\lambda(1 - 2\pi k^*/U_d^*) = \lambda - mc\eta$. The kinetic friction force therefore equals

$$F_0 \sim \lambda(1 - \pi k^*/U_d^*) = \lambda - mc\eta/2 \tag{66}$$

which, for small η, nearly equals λ, i.e. the kinetic friction is nearly equal to the static friction, and is independent of the sliding velocity. The latter is a consequence of the fact that independently of how small the driving velocity v is, rapid processes always occur during sliding.

Let us analyse the condition found above for an elastic instability to occur: $k\lambda > \rho c\eta$. When an elastic instability occurs the lattice at the defect performs local stick–slip motion. During 'stopping' an elastic stopping wave is emitted from the defect. The lattice atoms in the 'stopped' area exert a force on the defect which increases proportionally to the stopping time t (see the second term in (60)), which can be written as (using $F = m\eta v$)

$$F_{tot}(t) = \rho\eta cvt.$$

The force necessary for the lattice to go over the barrier at the defect equals λ. Thus the stopping time t_0 is determined by $F_{tot}(t_0) = \lambda$ or $\rho\eta cvt_0 = \lambda$. Comparing this equation with (65) gives $kvt_0 > 1$ as the condition for local stick–slip instability to occur. That is, no local stick–slip motion occurs if the force on the defect from the lattice reaches the pinning force λ during a time period which is shorter than the time that it takes for the lattice to move a distance $1/k = a/2\pi$. This condition is physically very appealing and should also be valid for 2D and 3D systems [12].

The picture above is modified at non-zero temperature. For $T > 0$ K, if v is low enough, the 'particle' will go over the barrier because of thermal excitation. If the velocity is very small the only role of the external spring force is to slightly 'tilt' the potential energy surface, leading to the 'particle' jumping slightly more often in the direction of the driving force than in the opposite direction. This results in 'creep motion', where the friction force depends linearly on the sliding velocity as $v \to 0$.

We close this section by presenting some numerical results which illustrate the analytical results given above. It is convenient to introduce a new time variable $\bar{t} = k^*t$ and define $\bar{U}_d = U_d^*/k^*$, $\bar{v} = v^*/k^*$, and $\bar{f} = f^*/k^*$. In these variables, equation (54) takes the form

$$\frac{\mathrm{d}X}{\mathrm{d}\bar{t}} = \bar{f} + (\bar{v}\bar{t} + X_0 - X) + \bar{U}_d \sin X$$

where

$$\langle \bar{f}(\bar{t})\bar{f}(0)\rangle = 2\bar{T}\delta(\bar{t})$$

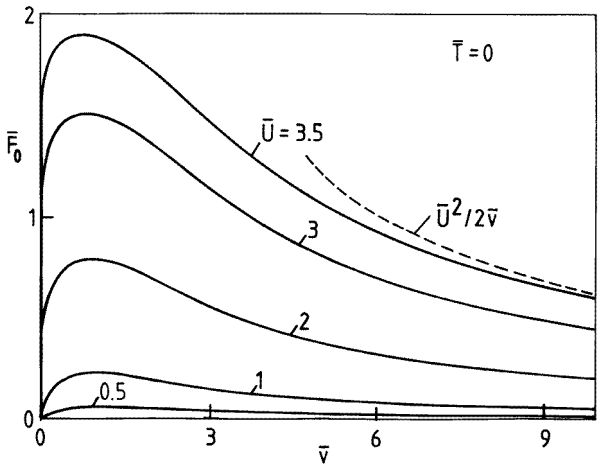

Figure 7. The dependence of the friction force, $\bar{F}_0 = -\langle \bar{U}_d \sin X \rangle$, on the sliding velocity v for different barrier heights. The dashed line indicates the high-velocity expansion (64) (which takes the form $\sim \bar{U}_d^2/2\bar{v}$ in the present units) for the case where $\bar{U}_d = 3.5$.

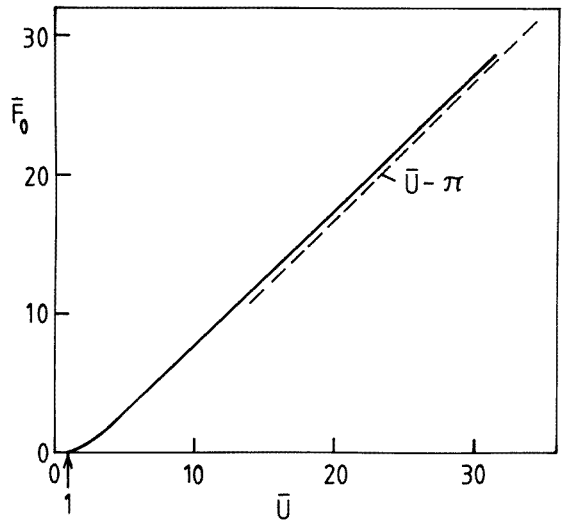

Figure 8. The friction force at low sliding velocity ($\bar{F}_0(0) = \lim_{\bar{v}\to 0} \bar{F}(\bar{v})$), as a function of the barrier height. The solid line is the exact result while the dashed line is the high-$\bar{U}_d$ expansion (equation (62)), which in the present units takes the form $\bar{F}_0 = \bar{U}_d - \pi$.

where $\bar{T} = T^*/k^*$. In the original variables $\bar{U}_d = 2U_d k^3 f(k)/\rho c \eta$ and $\bar{T} = 2k_B T k^2/\rho c \eta$. Figure 7 shows the dependence of the friction force $\bar{F}_0$ on the sliding velocity $\bar{v}$ for different barrier heights. For $\bar{U}_d > 1$ (i.e., $U_d^* > k^*$) an elastic instability occurs, and the friction force $F_0(0)$ is greater than zero, while it vanishes for $\bar{U}_d < 1$. The dashed line indicates the high-velocity expansion (64) (which takes the form $\sim \bar{U}^2/2\bar{v}$ in the present units) for the case where $\bar{U}_d = 3.5$. Figure 8 shows the friction force at low sliding velocity ($\bar{F}_0(0) = \lim_{v\to 0} \bar{F}_0(\bar{v})$) as a function of the barrier height. The solid line is the exact result while the dashed line is the high-$\bar{U}$ expansion (66), which in the present units takes the

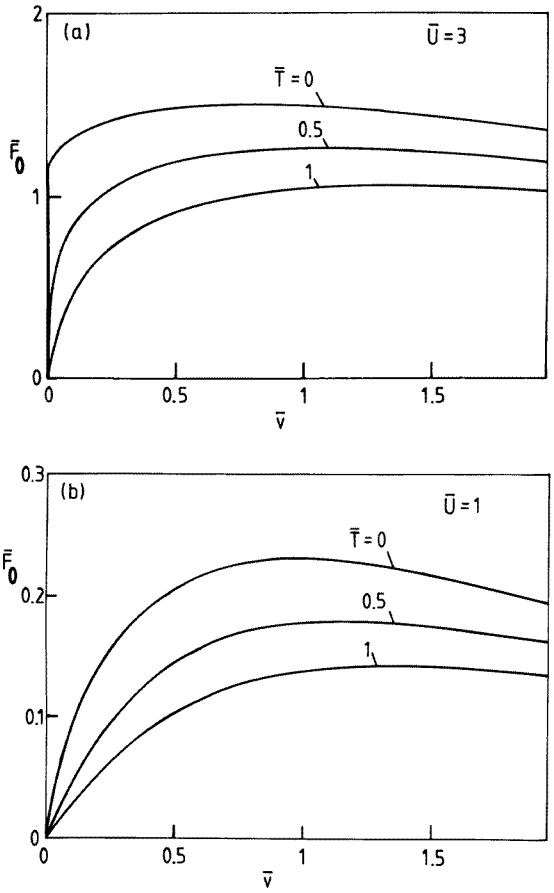

Figure 9. The temperature dependence of the relation between the friction force $\bar{F}_0$ and the sliding velocity $\bar{v}$ for (a) $\bar{U}_d = 3$ and (b) $\bar{U}_d = 1$.

form $\bar{F}_0 = \bar{U}_d - \pi$. Finally, figure 9 shows the relation between $\bar{F}_0$ and $\bar{v}$ for three different temperatures and for (a) $\bar{U}_d = 3$ and (b) $\bar{U}_d = 1$. In the former case, $\bar{F}(0)$ is non-zero when $\bar{T} = 0$, while it increases linearly with $\bar{v}$ (for small $\bar{v}$), for $\bar{T} > 0$. The results presented above may also be relevant for friction force microscopy; see reference [13].

6. Quartz crystal microbalance studies of the sliding friction

Sliding friction has been studied using the quartz crystal microbalance (QCM). In the measurements by Krim *et al* [5] two sides of a quartz crystal were covered by thin silver or gold films. When a voltage is applied to the crystal, it performs in-plane oscillations. If adsorbates are adsorbed on the metal film, the resulting mass load will decrease the resonance frequency of the oscillator. But Krim *et al* also observed an increased damping of the oscillator which can only result if, due to the inertia force, the adsorbates slide relative to the metal surface. In a typical experiment the oscillator frequency $\omega \sim 10^8$ s^{-1}, and the amplitudes of the adsorbate vibrations relative to the substrate are ~10–50 Å. The basic quantities deduced from the experimental data are the adsorbed mass mN (where N is the

number of adsorbed molecules), and the sliding friction $\bar{\eta}$ defined by (1).

Recent experimental and theoretical studies have shown that for a compressed incommensurate Xe monolayer on Ag(111) the sliding friction $\bar{\eta}$ may be dominated by the direct coupling between the sliding layer and the electronic excitations in the substrate [6, 7]. The main support for this claim comes from a comparison of the observed sliding friction with the electronic friction deduced from surface resistivity data. Assuming that this conclusion is correct, it remains to be understood why the corrugated substrate potential and the interaction with surface defects have a negligible influence on the sliding friction. The first question was addressed in reference [8], and below we consider the influence of surface defects on the sliding friction.

The force of inertia which acts on the adsorbate slab in a QCM measurement (which is the origin of why the slab will slide relative to the substrate) is extremely small, at least for thin adsorbate layers. This implies that the velocity is proportional to the driving force (linear response theory). To prove that a linear response is an excellent approximation, note that the force of inertia acting on an adsorbate is $F_{ext} \sim mA\omega_0^2$, where A is the vibration amplitude and ω_0 the vibration frequency of the quartz crystal. Using $A \sim 100$ Å and $\omega_0 \sim 10^8$ s^{-1} gives $F_{ext} \sim 10^{-8}$ eV Å^{-1} which is extremely small compared with the force due to the corrugated substrate potential or the potential from surface defects, which is of order U_d/a, where $a \sim 3$ Å is the length over which the pinning potential varies and $U_d \sim$ 1–10 meV is the strength of the defect potential. Thus $U_d/a \sim 10^{-3}$ eV Å$^{-1} \gg F_{ext}$, and the linear response approximation is very accurate.

Assume first zero temperature. A 2D elastic solid on a periodically corrugated substrate can be either pinned by the substrate potential, in which case a finite force (per particle) is necessary in order to start sliding, or else, if the amplitude of the substrate potential is small enough, no pinning occurs and the static friction force vanishes. On the other hand, if a *random* distribution of defects occur on the surface, the 2D solid will *always* be pinned by the defects. If the concentration of defects is very low one can neglect the interaction between the defects, and the total pinning force is the sum of the pinning forces from the (independent) pinning centres. However, the surfaces used in the QCM measurements have a relatively high concentration of defects. In these cases, if the interaction between the defects and the elastic solid is weak, pinning will occur via the formation of domains of linear size ξ; each domain can be considered as an 'effective' particle which is pinned individually. The effective particles experience a potential from the defects which is periodic and in the simplest case takes the form $U_1 \cos kx$ as a function of the coordinate x of the effective particle. The strength U_1 of the pinning potential and the linear size ξ of the domains is determined by the theory of Larkin and Ovchinnikov [14]. For a 2D solid of linear size L one has

$$\xi \approx \frac{mc^2 l}{U_d[4\pi \ln(L/\xi)]^{1/2}}$$

where $l = n_d^{-1/2}$ is of the order of the average distance between two nearby defects. In the present case, if $L \sim 1$ cm, $l \sim 100$ Å, and $U_d \sim 10$ meV, and using $mc^2 = 0.3$ eV as calculated for the compressed Xe monolayer on silver (see section 2), we get $\xi \approx 300$ Å. A 300 Å $\times$ 300 Å area contains approximately $N = 10^4$ Xe atoms on which the total external force $NF_{ext} \sim 10^{-5}$ eV Å^{-1} acts. This is much smaller than the pinning force which acts on a domain, which is of order kU_1, where the pinning barrier

$$U_1 \approx \xi U_d/l = mc^2/[4\pi \ln(L/\xi)]^{1/2}.$$

Using $mc^2 = 0.3$ eV gives $U_1 \approx 25$ meV and $kU_1 \sim 10$ meV Å$^{-1} \gg NF_{ext}$. Thus

no sliding motion is possible at zero temperature. However, for non-zero temperatures thermally activated motion (creep) will occur. Thermal excitation over the barrier U_1 depends on the ratio U_1/k_BT; for $U_1/k_BT \ll 1$ sliding occurs as if there were no barrier at all, in which case $\bar{\eta} \approx \eta$. But at low temperature $\bar{\eta} \sim \exp(2U_1/k_BT)$, and it is clear that by studying the temperature dependence of the sliding friction it is possible to deduce information about the pinning barrier. We urge our experimentalist colleagues to perform such temperature-dependent measurements.

It is interesting to note that the effective barrier U_1 depends logarithmically on the strength U_d of the defect potential, and is is thus very insensitive to the actual magnitude of U_d. For example, if U_d increases from 10 meV to 20 meV, U_1 increases by only ∼5%. This may be why the sliding friction for incommensurate solid Xe layers has been observed to be quite insensitive to the degree of surface perfection [15]. It is also interesting to note that the sliding friction $\bar{\eta}$ is independent of the sliding velocity [16] v, i.e., the friction force F_0 increases linearly with v. This is also consistent with the model of thermally activated (creep) motion described above. On the other hand, if the high-velocity expansion described in section 3 were to be valid, the defects would give a contribution to the friction force proportional to $\sim 1/v$. This could still be consistent with the experiments, but only if the contribution to $\bar{\eta}$ from the defects is negligible compared with the direct contribution η (which is velocity independent). To study this problem, let us assume that the sliding velocity $v \sim 1$ cm s^{-1}, and $n_d \sim 10^{-4}$ Å^{-2}. In this case, if we include only the smallest reciprocal-lattice vectors $G \sim 2\pi/a$ and assume that the decay constant $\alpha \sim 1/a^2$, then from (23) and (24)

$$\langle u^2 \rangle / a^2 \sim 1 \times 10^6 \, \mathrm{e}^{-2\pi^2} \sim 1 \times 10^{-3}$$

and

$$\bar{\eta} - \eta \sim 1 \times 10^{11} \, \mathrm{e}^{-2\pi^2} \ \mathrm{s}^{-1} \sim 1 \times 10^2 \ \mathrm{s}^{-1}.$$

This calculation indicates that the high-velocity expansion may, in fact, be valid, and that the contribution from the point defects to the friction force may be negligible. The results given above depend, however, very sensitively on the 'form factor' $f(G)$, and, e.g., a small change in the decay parameter α (see (6)) may change $\langle u^2 \rangle$ and $\bar{\eta} - \eta$ by several orders of magnitude.

The discussion above has only considered point defects, e.g., vacancies or adatoms. But for metallic surfaces the dominant imperfections may be steps. The influence of steps on the sliding friction is a complicated problem, since the steps are usually not straight and the distribution of steps not uniform. If the steps were to be straight and parallel to each other, and if the sliding direction were to be perpendicular to the steps, then the sliding dynamics at zero temperature would be equivalent to a 1D elastic solid interacting with a point defect. However, for non-zero temperatures this is no longer the case, and the 2D elastic properties of the system must be taken into account. Another limitation of the study above is the assumption of purely elastic deformations. For QCM friction studies of incommensurate Xe layers on Ag(111) this is an excellent approximation, since the driving force (per particle) is extremely weak (linear response), and the 2D elastic solid stiff, so no local shear melting or plastic deformation of the sliding lattice will occur in the vicinity of the surface defects (shear melting induced by defects has been observed in computer simulations for large driving forces (non-linear response); see reference [17]). Similarly, the force on a defect from the sliding lattice is so weak that no displacement of the defect will occur (at least not at zero temperature; for $T > 0$ K the defects may diffuse and

drift slowly in the direction of the sliding 2D solid, but even this effect is likely to be unimportant).

7. Summary and conclusions

We have studied the influence of defects on sliding friction. The leading contribution to the sliding friction at high sliding velocities and for small-amplitude vibrations has been derived for 1D, 2D, and 3D elastic solids. For a 1D solid with a low concentration of point defects we have presented an exact solution, valid for arbitrary temperature and strength of the defect potential. We have also discussed the role of defects in the linear (in the external driving force) sliding friction for Xe monolayers on metal surfaces. For this case we estimate the effective pinning barrier to be of the order of 25 meV. Thus one would expect a strong dependence of the sliding friction on temperature, and we urge our experimentalist colleagues to perform temperature-dependent measurements to test the theoretical predictions.

Acknowledgments

One of the authors (A I Volokitin) acknowledges financial support from the DFG and the Russian Foundation for Basic Research (Project No 96-02-16112).

Appendix A

In this appendix we discuss the sliding dynamics when $\eta = 0$. In this case, equation (53) takes the form

$$\frac{\mathrm{d}X}{\mathrm{d}t} = f^* + F^* + U_d^* \sin X. \tag{A1}$$

Thus we can interpret (A1) as the equation of motion of a particle in a periodic potential $U^*(X) = U_d^* \cos X$ under the influence of an external driving force F^* and a fluctuating force f^*. The motion is overdamped, since no $\mathrm{d}^2X/\mathrm{d}t^2$ term occurs in (A1). This problem has been solved exactly by Risken and Vollmer [18]. The drift velocity $\langle \mathrm{d}X/\mathrm{d}t\rangle = \mu F^*$, where the mobility μ in general depends on the driving force F^*, except for very small F^* (the linear response regime) where μ is independent of F^*. According to Risken and Vollmer

$$\mu = 2\pi(1 - \mathrm{e}^{-2\pi F^*/T^*})T^*\left[\int_0^{2\pi} \mathrm{d}x\ \mathrm{e}^{U^*(x)/T^*} \int_0^{2\pi} \mathrm{d}x\ \mathrm{e}^{-U^*(x)/T^*} - (1 - \mathrm{e}^{-2\pi F^*/T^*}) \int_0^{2\pi} \mathrm{d}x\ \mathrm{e}^{-U^*(x)/T^*} \int_0^{x} \mathrm{d}x'\ \mathrm{e}^{U^*(x')/T^*}\right]^{-1}. \tag{A2}$$

Note that $\mu \leqslant 1$. From (38) it is clear that the defect exerts a force on the elastic solid given by

$$F_0 = -\lambda\langle \sin k(vt - u)\rangle = -\lambda\langle \sin X\rangle. \tag{A3}$$

Using (A1) we get

$$\langle \sin X\rangle = [\langle \mathrm{d}X/\mathrm{d}t\rangle - F^*]/U_d^* = (\mu - 1)F^*/U_d^*. \tag{A4}$$

Thus

$$F_0 = 2\rho c v(1 - \mu). \tag{A5}$$

Consider now a low concentration of randomly distributed defects. If the distance between the defects is larger than c/η we can neglect the dynamical interaction between the defects. If N_d defects occur over the length L, and thus $n_d = N_d/L$, then the total friction force equals

$$Nm\bar{\eta}v = Nm\eta v + N_d F_0. \tag{A6}$$

Using (A5) this gives

$$\bar{\eta} = \eta + 2n_d c(1-\mu). \tag{A7}$$

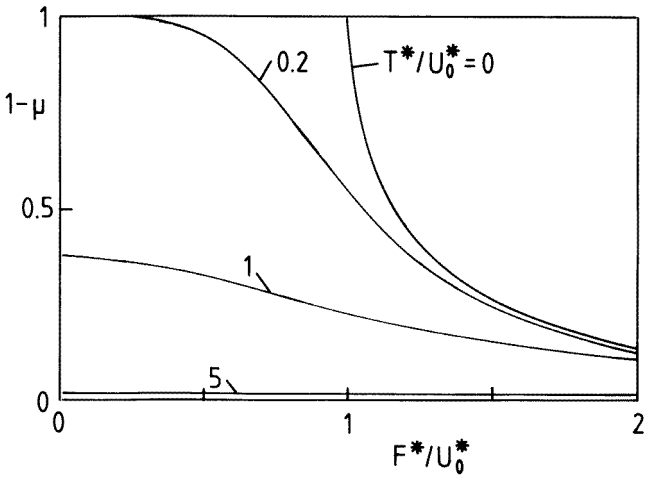

Figure A1. The friction coefficient, $1-\mu$, as a function of the driving force F^* for several different temperatures T^*. Based on reference [18].

Let us consider two limiting cases. Consider first zero temperature, where (A2) reduces to

$$\mu = \left[1 - (U_d^*/F^*)^2\right]^{1/2} \qquad \text{for } |F^*| > U_d^* \tag{A8}$$

and zero otherwise. Since $U_d^*/F^* = U_d k^2 f(k)/\rho c v$ we get

$$\bar{\eta} = \eta + 2n_d c \qquad \text{if } v < U_d k^2 f(k)/\rho c \tag{A9}$$

and

$$\bar{\eta} = \eta + 2n_d c(1 - [1 - (U_d k^2 f(k)/\rho c v)^2]^{1/2}) \qquad \text{if } v > U_d k^2 f(k)/\rho c. \tag{A10}$$

Note that the first limit is identical to the result obtained earlier for small-amplitude low-frequency vibrations; see (33). In the high-velocity limit, equation (A10) gives to leading order in $1/v$

$$\bar{\eta} = \eta + n_d c\left(\frac{U_d k^2 f(k)}{\rho c v}\right)^2. \tag{A11}$$

This result is identical to (25) if in the sum over G in (25) we only include the two lowest (non-vanishing) terms, $G = \pm k$, as was done in the derivation of the effective potential U (see (14)).

As a second important limit, let us consider a linear response where F^* (i.e. v) is very small. In this case (A2) reduces to

$$\mu = \left(2\pi \Big/ \int_0^{2\pi} \mathrm{d}x \ \mathrm{e}^{(U_d^*/T^*)\cos x} \right)^2 . \tag{A12}$$

Thus

$$\bar{\eta} = \eta + n_d c \left[1 - \left(2\pi \Big/ \int_0^{2\pi} \mathrm{d}x \ \mathrm{e}^{(U_d^*/T^*)\cos x} \right)^2 \right] . \tag{A13}$$

Let us assume that $U_d^*/T^* \ll 1$. In this case (A13) reduces to

$$\bar{\eta} = \eta + n_d c \left(\frac{U_d k f(k)}{k_B T} \right)^2 . \tag{A14}$$

Figure 10 shows the friction factor $1-\mu$ as a function of F^*/U^* for several temperatures.

References

[1] See, e.g.,
Kardar M and Ertas D 1995 *Scale Invariance, Interfaces, and Non-equilibrium Dynamics* ed A McKane, M Droz, J Vannimenus and D Wolf (New York: Plenum) and references therein
[2] See, e.g., articles in
Persson B N J and Tosatti E (ed) 1996 *Physics of Sliding Friction* (Dordrecht: Kluwer)
[3] Blatter G, Feigelman M V, Geshkenbein V B, Larkin A I and Vinokur V M 1994 *Rev. Mod. Phys.* **66** 1125
[4] Grüner G 1988 *Rev. Mod. Phys.* **60** 1129
[5] Krim J, Solina D H and Chiarello R 1991 *Phys. Rev. Lett.* **66** 181
[6] Persson B N J and Volokitin A I 1995 *J. Chem. Phys.* **103** 8679
See also,
Schaich W L and Harris J 1981 *J. Phys. F: Met. Phys.* **11** 65
Sokoloff J B 1995 *Phys. Rev.* B **52** 5318
[7] Krim J and Daly C 1997 to be published
[8] Persson B N J and Nitzan A 1996 *Surf. Sci.* **367** 261
[9] Sokoloff J B 1995 *Phys. Rev.* B **51** 15 573
[10] Persson B N J and Ryberg R 1985 *Phys. Rev.* B **32** 3586
[11] Rozman M G, Urbakh M and Klafer J 1996 *Phys. Rev. Lett.* **77** 683
Cule D and Hwa T 1996 *Phys. Rev. Lett.* **77** 278
Coppersmith S N 1990 *Phys. Rev. Lett.* **65** 1044
Elmer F J, Matsukawa H and Fukuyama H 1996 *Physics of Sliding Friction* ed B N J Persson and E Tosatti (Dordrecht: Kluwer)
[12] Persson B N J and Volokitin A I 1997 to be published
[13] Gyalog T, Bammerlin M, Lüthi R, Meyer E and Thomas H 1995 *Europhys. Lett.* **31** 269
[14] Larkin A I and Ovchinnikov Yu N 1979 *J. Low Temp. Phys.* **34** 409
[15] Krim J and Daly C 1996 *Physics of Sliding Friction* ed B N J Persson and E Tosatti (Dordrecht: Kluwer)
[16] Krim J, private discussion
[17] Persson B N J 1995 *J. Chem. Phys.* **103** 3849
[18] Risken H and Vollmer H D 1979 *Phys. Lett.* **69A** 387